Hole injection and electron overflow improvement in InGaN/GaN light-emitting diodes by a tapered AlGaN electron blocking layer

Bing-Cheng Lin,[1] Kuo-Ju Chen,[1] Chao-Hsun Wang,[1] Ching-Hsueh Chiu,[2] Yu-Pin Lan,[1] Chien-Chung Lin,[3] Po-Tsung Lee,[1] Min-Hsiung Shih,[1] Yen-Kuang Kuo,[4] and Hao-Chung Kuo[1,*]

[1]*Department of Photonics and Institute of Electro-Optical Engineering, National Chiao Tung University, Hsinchu 30010, Taiwan*
[2]*Advanced Optoelectronic Technology Inc., No. 13, Gongye 5th Rd., Hukou Township, Hsinchu County 303, Taiwan*
[3]*Institute of Photonics System, National Chiao Tung University, Tainan 71150, Taiwan*
[4]*Department of Physics, National Changhua University of Education, Changhua 500, Taiwan*
**hckuo@faculty.nctu.edu.tw*

Abstract: A tapered AlGaN electron blocking layer with step-graded aluminum composition is analyzed in nitride-based blue light-emitting diode (LED) numerically and experimentally. The energy band diagrams, electrostatic fields, carrier concentration, electron current density profiles, and hole transmitting probability are investigated. The simulation results demonstrated that such tapered structure can effectively enhance the hole injection efficiency as well as the electron confinement. Consequently, the LED with a tapered EBL grown by metal-organic chemical vapor deposition exhibits reduced efficiency droop behavior of 29% as compared with 44% for original LED, which reflects the improvement in hole injection and electron overflow in our design.

©2014 Optical Society of America

OCIS codes: (230.3670) Light-emitting diodes; (230.2090) Electro-optical devices.

References and links

1. S. Nakamura, M. Senoh, N. Iwsa, and S.-I. Nagahama, "High-brightness InGaN blue, green and yellow light-emtting diodes with quantum well structures," Jpn. J. Appl. Phys. **34**(Part 2, No. 7A), L797–L799 (1995).
2. Y. Taniyasu, M. Kasu, and T. Makimoto, "An aluminium nitride light-emitting diode with a wavelength of 210 nanometres," Nature **441**(7091), 325–328 (2006).
3. M.-H. Kim, M. F. Schubert, Q. Dai, J. K. Kim, E. F. Schubert, J. Piprek, and Y. Park, "Origin of efficiency droop in GaN-based light-emitting diodes," Appl. Phys. Lett. **91**(18), 183507 (2007).
4. K. J. Vampola, M. Iza, S. Keller, S. P. DenBaars, and S. Nakamura, "Measurement of electron overflow in 450 nm InGaN light-emitting diode structures," Appl. Phys. Lett. **94**(6), 061116 (2009).
5. C. H. Wang, J. R. Chen, C. H. Chiu, H. C. Kuo, Y. L. Li, T. C. Lu, and S. C. Wang, "Temperature-dependent electroluminescence efficiency in blue InGaN–GaN light-emitting diodes with different well widths," IEEE Photon. Technol. Lett. **22**(4), 236–238 (2010).
6. A. David and M. J. Grundmann, "Droop in InGaN light-emitting diodes: A differential carrier lifetime analysis," Appl. Phys. Lett. **96**(10), 103504 (2010).
7. B. Monemar and B. E. Sernelius, "Defect related issues in the "current roll-off" in InGaN based light emitting diodes," Appl. Phys. Lett. **91**(18), 181103 (2007).
8. X. Ni, Q. Fan, R. Shimada, Ü. Özgür, and H. Morkoç, "Reduction of efficiency droop in InGaN light emitting diodes by coupled quantum wells," Appl. Phys. Lett. **93**(17), 171113 (2008).
9. R. A. Arif, Y.-K. Ee, and N. Tansu, "Polarization engineering via staggered InGaN quantum wells for radiative efficiency enhancement of light-emitting diodes," Appl. Phys. Lett. **91**(9), 091110 (2007).
10. H. Zhao, G. Liu, J. Zhang, J. D. Poplawsky, V. Dierolf, and N. Tansu, "Approaches for high internal quantum efficiency green InGaN light-emitting diodes with large overlap quantum wells," Opt. Express **19**(S4 Suppl 4), A991–A1007 (2011).
11. R. M. Farrell, E. C. Young, F. Wu, S. P. DenBaars, and J. S. Speck, "Materials and growth issues for high-performance nonpolar and semipolar light-emitting devices," Semicond. Sci. Technol. **27**(2), 024001 (2012).

#195065 - $15.00 USD Received 23 Aug 2013; revised 11 Oct 2013; accepted 14 Oct 2013; published 3 Jan 2014
(C) 2014 OSA

12. P. S. Hsu, M. T. Hardy, F. Wu, I. Koslow, E. C. Young, A. E. Romanov, K. Fujito, D. F. Feezell, S. P. DenBaars, J. S. Peck, and S. Nakamura, "444.9 nm semipolar (11 $\bar{2}$ 2) laser diode grown on an intentionally stress relaxed InGaN waveguiding layer," Appl. Phys. Lett. **100**, 021104 (2012).
13. M. F. Schubert, J. Xu, J. K. Kim, E. F. Schubert, M. H. Kim, S. Yoon, S. M. Lee, C. Sone, T. Sakong, and Y. Park, "Polarization-matched GaInN/AlGaInN multi-quantum-well light-emitting diodes with reduced efficiency droop," Appl. Phys. Lett. **93**(4), 041102 (2008).
14. P.-M. Tu, C.-Y. Chang, S.-C. Huang, C.-H. Chiu, J.-R. Chang, W.-T. Chang, D.-S. Wuu, H.-W. Zan, C.-C. Lin, H.-C. Kuo, and C.-P. Hsu, "Investigation of efficiency droop for InGaN-based UV light-emitting diodes with InAlGaN barrier," Appl. Phys. Lett. **98**(21), 211107 (2011).
15. H. Zhao, G. Liu, R. A. Arif, and N. Tansu, "Current injection efficiency induced efficiency-droop in InGaN quantum well light-emitting diodes," Solid-State Electron. **54**(10), 1119–1124 (2010).
16. Y.-K. Kuo, J.-Y. Chang, M.-C. Tasi, and S.-H. Yen, "Advantages of blue InGaN multiple-quantum well light-emitting diodes with InGaN barriers," Appl. Phys. Lett. **95**(1), 011116 (2009).
17. C. H. Wang, C. C. Ke, C. Y. Lee, S. P. Chang, W. T. Chang, J. C. Li, Z. Y. Li, H. C. Yang, H. C. Kuo, T. C. Lu, and S. C. Wang, "Hole injection and efficiency droop improvement in InGaN/GaN light-emitting diodes by band-engineered electron blocking layer," Appl. Phys. Lett. **97**(26), 261103 (2010).
18. Y.-K. Kuo, M.-C. Tasi, and S.-H. Yen, "Numerical simulation of blue InGaN light-emitting diodes with polarization-matched AlGaInN electron-blocking layer and barrier layer," Opt. Commun. **282**(21), 4252–4255 (2009).
19. W. Yang, D. Li, J. He, and X. Hu, "Advantage of tapered and graded AlGaN electron blocking layer in InGaN-based blue laser diodes," Phys. Status Solidi C **10**(3), 346–349 (2013).
20. W. Yang, D. Li, N. Liu, Z. Chen, L. Wang, L. Liu, L. Li, C. Wan, W. Chen, X. Hu, and W. Du, "Improvement of hole injection and electron overflow by a tapered AlGaN electron blocking layer in InGaN-based laser diodes," Appl. Phys. Lett. **100**(3), 031105 (2012).
21. Y. Zhang, T.-T. Kao, J. Liu, Z. Lochner, S.-S. Kim, J.-H. Ryou, R. D. Dupuis, and S.-C. Shen, "Effects of a step-graded $Al_xGa_{1-x}N$ electron blocking layer in InGaN-based laser diodes," J. Appl. Phys. **109**(8), 083115 (2011).
22. APSYS by Crosslight Software Inc, Burnaby, Canada, http://www.crosslight.com.
23. J. Piprek and S. Nakamura, "Physics of high-power InGaN/GaN lasers," in *Proceedings of IEE Conference on Optoelectron.* (2002), pp. 145–151.
24. J. Piprek, "Ultra-violet light-emitting diodes with quasi acceptor-free AlGaN polarization doping," Opt. Quantum Electron. **44**(3-5), 67–73 (2012).
25. I. Vurgaftman and J. R. Meyer, "Band parameters for nitrogen-containing semiconductors," J. Appl. Phys. **94**(6), 3675–3696 (2003).
26. J.-R. Chen, C.-H. Lee, T.-S. Ko, Y.-A. Chang, T.-C. Lu, H.-C. Kuo, Y.-K. Kuo, and S.-C. Wang, "Effects of built-in polarization and carrier overflow on InGaN quantum-well lasers with electron blocking layers," J. Lightwave Technol. **26**(3), 329–337 (2008).
27. H. J. Kim, S. Choi, S.-S. Kim, J.-H. Ryou, P. D. Yoder, R. D. Dupuis, A. M. Fischer, K. Sun, and F. A. Ponce, "Improvement of quantum efficiency by employing active-layer-friendly lattice-matched InAlN electron blocking layer in green light-emitting diodes," Appl. Phys. Lett. **96**(10), 101102 (2010).
28. V. Fiorentini, F. Bernardini, and O. Ambacher, "Evidence for nonlinear macroscopic polarization in III-V nitride alloy heterostructures," Appl. Phys. Lett. **80**(7), 1204–1206 (2002).

1. Introduction

III-nitride light-emitting diodes (LEDs) have various applications due to its widely tunable wavelength from ultraviolet to blue/green [1,2], and have been in the center of lighting research due to their high efficiencies. However, the internal quantum efficiency (IQE) of the InGaN LEDs usually reaches a maximum value at low current density and then droops remarkably with the increase of current density [3,4]. Various possible mechanisms of this efficiency droop including electron overflow out of the active region, nonuniform distribution of holes, Auger scattering, carrier delocalization, poor hole injection have been proposed [4–7]. Among these factors, electron overflow and poor hole injection might be the main mechanisms in GaN-based blue LEDs [4,8]. In recent years, great efforts have been made to overcome the efficiency droop problem. Some of groups focus on increasing electron-hole wavefunction overlap by solving charge separation issue in the active region, such as using staggered InGaN well [9,10] and non/semi-polar InGaN/GaN LEDs [11,12]. Schubert *et al*. and Tu *et al*. have employed the polarization-matched AlGaInN barriers in LEDs and achieved reduction of carrier leakage [13,14]. Zhao *et al*. proposed that when the thin layers of larger bandgap AlGaN barriers were employed, the efficiency droop phenomenon could be suppressed slightly [15]. To enhance electrons confinement and suppress the leaked electrons, a high-bandgap $Al_{1-x}Ga_xN$ electron blocking layer (EBL) is usually inserted between the

#195065 - $15.00 USD Received 23 Aug 2013; revised 11 Oct 2013; accepted 14 Oct 2013; published 3 Jan 2014
(C) 2014 OSA

active layer and the p-type layer. However, it has been reported that the large polarization field in $Al_{1-x}Ga_xN$ EBL reduces the effective potential height for electrons. On the other hand, the injection of holes could be difficult owing to low mobility, high effective mass, and downward band-bending induced by the serious polarization at the interface between the last quantum barrier (QB) of the multiple quantum wells (MQWs) and EBL [13], [16]. Several suggestions about the designs of EBL have been reported, including employing graded-composition EBL [17] and adopting the polarization-matched AlGaInN EBL [18]. However, these designs are difficult to grow, and the crystal quality of the subsequent p-GaN layer will be degraded. Recently published studies point out that a tapered AlGaN EBL with step-graded Al content in their laser diodes (LDs) with lower threshold current density and higher slope efficiency [19–21]. Therefore, taking the growth quality into consideration, a tapered four-layer AlGaN EBL in InGaN/GaN LED is proposed and investigated in this work.

2. Experiments and simulations

The epitaxial InGaN/GaN LED structures with conventional EBL and tapered EBL were grown on c-plane sapphire substrate by metal-organic chemical vapor deposition (MOCVD). After depositing a low temperature GaN nucleation layer, a 2.6-μm-thick undoped GaN layer, and a 4-μm-thick n-type GaN layer (n-doping = 1.5×10^{19} cm^{-3}) were grown. On the top of the buffer layer, eight-period 3-nm-thick $In_{0.19}Ga_{0.81}N$ quantum wells (QWs) sandwiched by nine 14-nm-thick n-type GaN barrier layers (n-doping = 1.1×10^{17} cm^{-3}) were grown, followed by a 50-nm-thick p-$Al_{0.16}Ga_{0.84}N$ EBL (p-doping = 5×10^{17} cm^{-3}) and a 150-nm-thick p-type GaN cap layer (p-doping = 1×10^{18} cm^{-3}). For comparison, the EBL of the original LED is a single p-$Al_{0.16}Ga_{0.84}N$ layer, and that of the tapered EBL LED was formed by replacing the last 14 nm QB by a 4 nm p-$Al_{0.04}Ga_{0.96}N$ layer, followed by a 5 nm p-$Al_{0.08}Ga_{0.92}N$ layer, and a 5 nm p-$Al_{0.12}Ga_{0.88}N$ layer (p-doping = 2×10^{16} cm^{-3} for the three layers), while the single p-$Al_{0.16}Ga_{0.84}N$ layer was unchanged. The major difference in the EBL design comes from the variation in the transition of the last QB to the $Al_{0.16}Ga_{0.84}N$ EBL. The growth temperature of conventional EBL and tapered four-layer AlGaN EBL was the same (1030 °C). During the growth of AlGaN, the flow rates of trimethylaluminium (TMAl) with Al = 4%, 8%, and 12% were 1.15, 2.36, and 3.76 μmol/min, respectively. The flow rates of trimethylgallium (TMGa), ammonia (NH_3), and bis cyclopentadienyl magnesium (Cp_2Mg) were 27.3, 0.12, and 0.127 μmol/min, respectively. On the other hand, the activation temperature and time condition of the p-type doping for the EBL were 760 °C and 20 minutes by nitrogen ambient thermal annealing treatment. The Mg doping concentrations in the p-type layer, AlGaN EBL were determined from the measurement of the secondary ion mass spectrometry (SMIS) and the Al composition in AlGaN was estimated by performing HRXRD measurement. Subsequently, the LED mesa with an area 300×300 μm^2 was defined by using standard photolithography and dry etching. In addition, a transparent conduction indium-tin-oxide (ITO) layer was employed to be the current spreading layer and Ni/Au metal was deposited as p-type and n-type electrodes, respectively. The emission wavelengths of both LEDs were around 450 nm.

Prior to the actual fabrication of devices, the band diagrams, electrostatic fields, carrier distributions, and electron current density profiles, and hole transmitting probability of the LEDs are first evaluated by APSYS (advance physical model of semiconductor devices) simulation software [22]. The APSYS simulation program is based on 2-D models and can deal with optical and electrical properties of the LED devices. The structures, such as layer thicknesses, doping concentrations, and Al composition are the same as the actual devices. Commonly accepted physical parameters were adopted to perform the simulations, the Shockley-Read-Hall (SRH) recombination lifetime of 10 ns, and the Auger recombination coefficient in QWs with order of 10^{-31} cm^6/s, respectively. The interface charge densities caused by spontaneous and piezoelectric polarization are calculated by assuming a screening factor of 50%. The band-offset ratios are assumed to be 0.7/0.3 and 0.5/0.5 for InGaN and

#195065 - $15.00 USD Received 23 Aug 2013; revised 11 Oct 2013; accepted 14 Oct 2013; published 3 Jan 2014
(C) 2014 OSA

AlGaN, respectively [23,24]. We use an Mg activation energy of 170 meV for GaN which is assumed to increase by 3 meV per % Al for AlGaN. Other material parameters used in the simulation can be found in [25].

3. Results and discussions

The calculated energy band diagram of original LED at 200 mA is shown in Fig. 1. The positions of the eight QWs are marked with gray areas. Severe band-banding occurs within the active region, i.e., sloped triangular barriers and wells, are observed in the original LED, as shown in Fig. 1(a). As shown in Fig. 1(b), an unintentional suppression of conduction band edge is obvious at the interface of last-QB/EBL. This dip is under electron quasi-Fermi level and thus electrons would accumulate at this interface. Under this circumstance, a severe electron overflow could be expected, which degrades the quantum efficiency of light emitter devices [26,27]. As shown in Fig. 1(c), it is apparent that the polarization-induced band-bending at the interface of last-QB/EBL is downward, which increase the difficulty for the holes to transport into the active region.

The built-in charge density induced by spontaneous and piezoelectric polarizations within the interface of the InGaN/GaN LED can be calculated by the method developed by Fiorentini

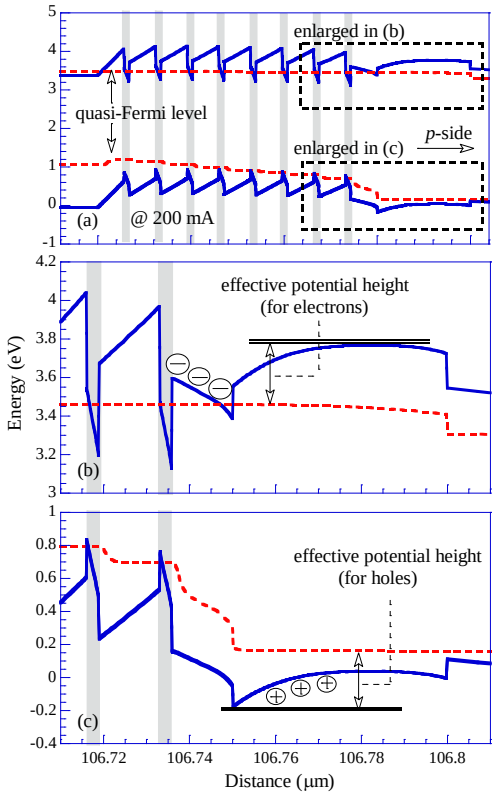

Fig. 1. (a) Energy band diagram of the original LED at 200 mA. (b) Enlarged drawing of the conduction band near the last-QB/EBL interface. (c) Enlarged drawing of the valance band near the last-QB/EBL interface.

#195065 - $15.00 USD Received 23 Aug 2013; revised 11 Oct 2013; accepted 14 Oct 2013; published 3 Jan 2014
(C) 2014 OSA

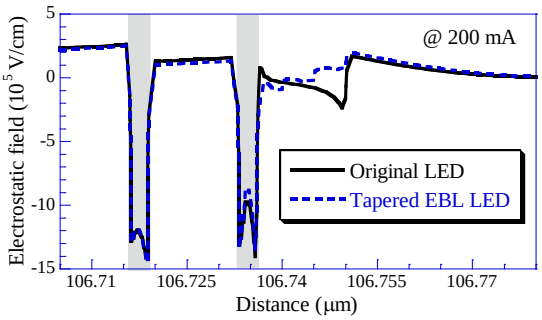

Fig. 2. Electrostatic fields near the last two QWs and EBL for original and tapered EBL LEDs at 200 mA.

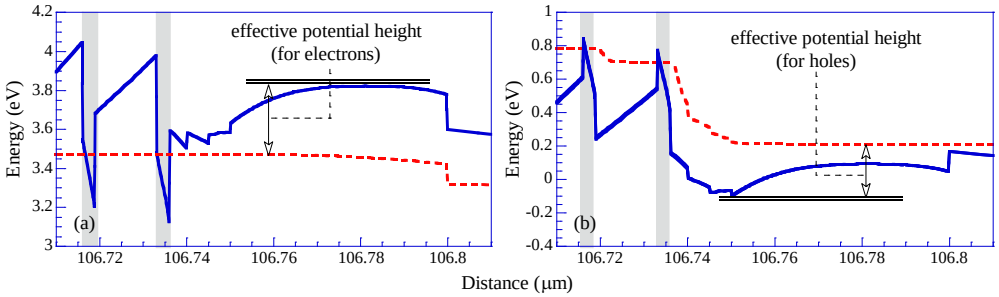

Fig. 3. Enlarged energy band diagrams near the last-QB/EBL interface of tapered EBL LED in (a) the conduction band (b) the valance band at 200 mA.

et al. [28]. For the tapered EBL LED, as compared with the original LED, the polarization induced surface charge density in the last-QW/last-QB interface increases (7.48×10^{16} m^{-2} versus 6.69×10^{16} m^{-2}), while that in the last-QB/EBL interface decreases (3.15×10^{16} m^{-2} versus 6.78×10^{15} m^{-2}). The use of the tapered EBL instead of conventional EBL can diminish the polarization charges accumulated in the last-QB/EBL interface, which accordingly can relax the band banding of EBL. Figure 2 show the electrostatic fields of original and tapered EBL LEDs near the last two QWs and EBL at 200 mA. Evidently, the original LED possesses a much stronger electrostatic field at the last-QB/EBL interface because of high surface charge density. Furthermore, smaller electrostatic field at the last-QB/EBL interface is also observed in tapered EBL LED due to the strain-induced polarization charge being spatially re-distributed. As shown in Fig. 2, there are stronger electrostatic fields in the active regions of original LED especially for the last QW, which may lead to the band bending, poor overlap of electron and hole wave functions, and hence reduced radiative recombination rate. Moreover, the weaker electrostatic fields in the active regions are observed for the tapered EBL LED. For this reason, the tapered EBL LED has higher radiative recombination rate than that of the original LED.

Figure 3 shows the enlarged energy band diagrams near the last-QB/EBL interface of tapered EBL LED at 200 mA. As shown in Fig. 3(a) the conduction band offset at the interface is small due to the stepped aluminium composition of tapered EBL LED. Consequently, the small dip lies high above the electron quasi-Fermi level. As indicated in Fig. 3(b), because of the smaller electrostatic field, the downward band-bending at the interface near EBL of tapered EBL LED is slighter than that of the original LED, which will lead to enhancement of hole injection efficiency.

Figure 4 shows the calculated electron and hole distributions within the active regions for original and tapered EBL LEDs at 200 mA. In Fig. 4(a), more severe electron accumulation at the last-QB/EBL interface caused by band bending can be found obviously in original LED.

#195065 - $15.00 USD Received 23 Aug 2013; revised 11 Oct 2013; accepted 14 Oct 2013; published 3 Jan 2014
(C) 2014 OSA

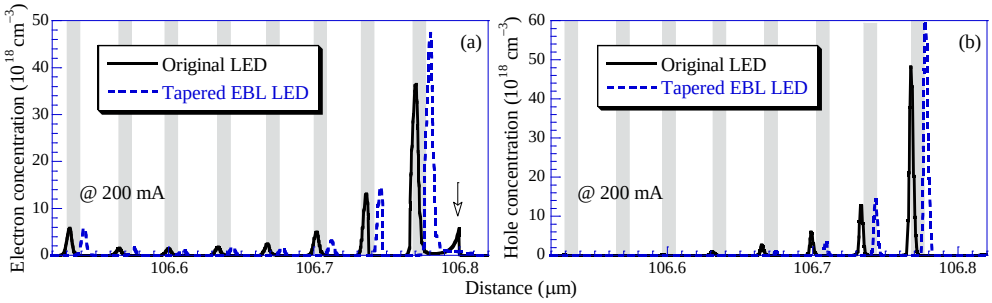

Fig. 4. (a) Electron and (b) hole concentrations within the active regions for original and tapered EBL LEDs at 200 mA.

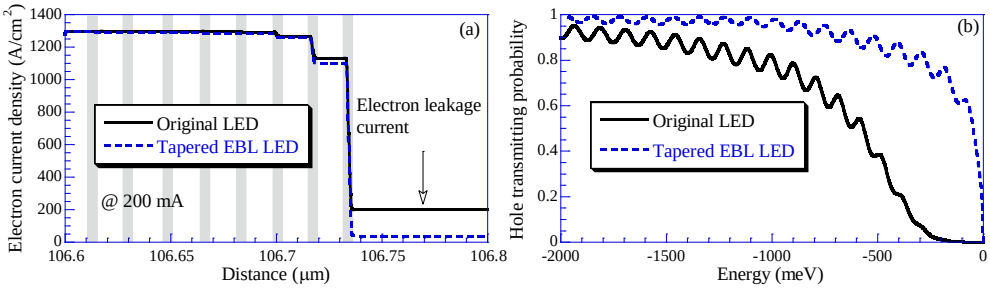

Fig. 5. (a) Electron current density profiles near the active regions and (b) hole transmitting probability near the last QB and EBL for original and tapered EBL LEDs.

However, the electron accumulation disappears in tapered EBL LED. As shown in Figs. 1(b) and 1(c), the effective potential height for electrons at the conduction band near the last QB and the EBL of original LED (308 meV) is smaller than that of the tapered EBL LED, and accordingly, its effective potential height for holes at the valance band (355 meV) is larger. As a result, the original LED has bad electron confinement and hole injection efficiency. The electron and hole concentrations in the active region of original LED are smaller than that of the tapered EBL LED, as shown in Fig. 4. Tapered EBL LED, with a special designed last QB, has slighter band bending. As shown in Figs. 3(a) and 3(b), it has higher effective potential height for electrons of 410 meV and lower effective potential height for holes of 290 meV. Thus, tapered EBL LED has higher electron and hole concentrations in the MQWs due to excellent electron confinement and higher hole injection efficiency.

Figure 5(a) shows the electron current density profiles near the active regions for original and tapered EBL LEDs at 200 mA. The electron current density and the electron concentration are connected by drift-diffusion model. The electron current is injected from n-type layers into QWs and recombines with holes, which results in the decrease of electron current density. Electron current overflow across the EBL is considered as the leakage current. As shown in Fig. 5(a), electron leakage current can be suppressed by employing the tapered EBL LED. This result shows that the tapered EBL structure is also an efficient electron blocker for InGaN/GaN LEDs. Figure 5(b) shows the tunneling probability of holes with respect to hole energy near the last QB and EBL for original and tapered EBL LEDs. Note that the negative energy corresponds to the hole transport. As shown in Fig. 5(b), the transmitting probability of holes for tapered EBL LED is larger than that of the original LED, especially for hole energy is low.

Finally, the devices with such designs are fabricated by regular LED process procedures, and the measured external quantum efficiencies (EQEs) under various currents are shown in Fig. 6. It can be seen that the experimental data have similar droop behavior to simulation results. However, the efficiency of tapered EBL LED shows slightly lower value in experime-

#195065 - $15.00 USD Received 23 Aug 2013; revised 11 Oct 2013; accepted 14 Oct 2013; published 3 Jan 2014
(C) 2014 OSA

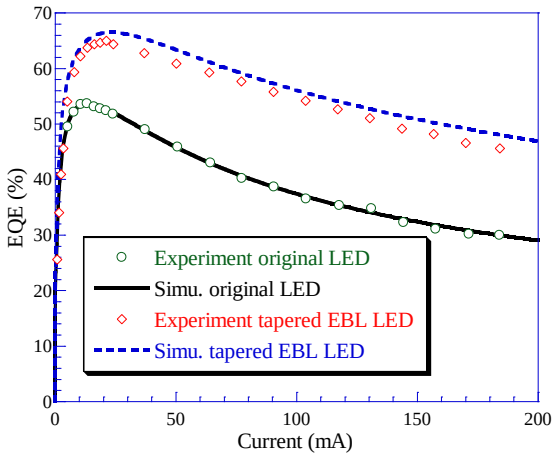

Fig. 6. Experiment and simulation external quantum efficiency for original and tapered EBL LEDs.

nt. This could be attributed to non-optimized epitaxial parameters. According to Fig. 6, the original LED has serious efficiency droop. Tapered EBL LED shows significantly mitigated efficiency droop. The efficiency droop was reduced from 44% in original LED to 29% in tapered EBL LED. This result confirms that the tapered EBL design did contribute to reduce the efficiency droop. This significant improvement in efficiency can be mainly attributed to the enhancement of hole injection as well as electron confinement, especially at high injection current.

4. Conclusion

When the tapered EBL structure is used, the hole injection efficiency into the active region can be increased, and the electron overflow can be significantly reduced. The physical origin for the performance improvement could be attributed to the mitigated downward band bending and the higher effective potential height for electrons. The tapered EBL LED was realized by MOCVD, and the efficiency droop was reduced from 44% in original LED to 29% in tapered EBL LED.

Acknowledgments

This work was funded by the National Science Council in Taiwan under grant number, NSC102-3113-P-009-007-CC2 and NSC-102-2221-E-009-131-MY3.